A Multiobjective Minimax Regret Robust VAr Planning Model

Julio López, *Member, IEEE*, David Pozo, *Student Member, IEEE*, Javier Contreras, *Fellow, IEEE*, and Jose Roberto Sanches Mantovani, *Member, IEEE*

***Abstract*—This paper proposes a risk-based mixed integer quadratically-constrained programming model for the long-term VAr planning problem. Risk aversion is included in the proposed model by means of regret-based optimization to quantify the load shedding risk because of a reactive power deficit. The expected operation and expansion costs of new installed reactive power sources and load shedding risk are jointly minimized. Uncertainty in the active and reactive load demands has been included in the model. An ϵ-constraint approach is used to characterize the optimal efficient frontier. Also, discrete tap settings of tap-changing transformers are modeled as a set of mixed integer linear equations which are embedded into an ac optimal convex power flow. Computational results are obtained from a realistic South and South–East Brazilian power system to illustrate the proposed methodology. Finally, conclusions are duly drawn.**

***Index Terms*—Discrete tap settings, load shedding, multiobjective, quadratically-constrained, regret optimization, risk, uncertainties.**

NOMENCLATURE

The following notation is used throughout the paper:

Indexes

h	Index of steps of tap-changing transformers.
i, j	Index of buses of the system.
t	Index of periods.
ω	Index of scenarios.

Sets

$\mathcal{E}$	Set of existing shunt reactive power sources.
$\mathcal{G}$	Set of generation units.
$\mathcal{K}$	Set of candidate buses to install new reactive power sources.
$\mathcal{L}$	Set of transmission lines.
$\mathcal{M}$	Set of steps of tap-changing transformers.
$\mathcal{N}$	Set of buses of the system.
$\mathcal{P}$	Set of periods.
$\mathcal{PQ}$	Set of load demand buses.
$\mathcal{T}$	Set of ULTC transformers.
$\mathcal{Z}$	Set of integer numbers.
Ω	Set of scenarios.

Parameters

B	Reactive power expansion budget.
C_i^{fix}	Fixed cost of candidate reactive power source in bus i.
C_i^{op}	Operating cost of candidate reactive power source in bus i.
C_i^{ls}	Load shedding cost in bus i.
I_t	Annual interest rate in each period t.
P_{G_i}	Active power produced by generation unit i.
$Q_{G_i}^{\min}, Q_{G_i}^{\max}$	Lower and upper reactive power limits of generation unit i.
$Q_{P_i}^{\max}, Q_{N_i}^{\max}$	Reactive capacitive and inductive power limits of candidate reactive power source in bus i.
$Q_{\text{SH}_\text{i}}^{\min}, Q_{\text{SH}_\text{i}}^{\max}$	Lower and upper limits of an existing reactive power source in bus i.
R_{ij}	Regulation range of tap-changing transformer ij.
S_{ij}	Total number of discrete steps of tap-changing transformer ij.
$S_{\text{ij}}^{\max}$	MVA capacity limit of branch ij.
$T_{\text{ij}}^{\min}, T_{\text{ij}}^{\max}$	Lower and upper tap limits of tap-changing transformer ij.
$V_i^{\min}, V_i^{\max}$	Lower and upper voltage magnitude in bus i.
ϵ	Auxiliary parameter to compute the voltage angle constraint.
$P_{D\,i,t}(\omega)$	Active load demand in bus i, in period t, depending on scenario ω.
$Q_{D\,i,t}(\omega)$	Reactive load demand in bus i, in period t, depending on scenario ω.
$\pi(\omega)$	Probability of scenario ω.
$\rho_t(\omega)$	Number of hours in each period t and scenario ω.

First-Stage Variables

$p_{G_{i,t}}^{\text{sl}}$	Active power generation in `slack` bus i and period t.

Manuscript received November 12, 2015; revised March 7, 2016 and June 21, 2016; accepted September 20, 2016. Date of publication September 27, 2016; date of current version April 17, 2017. This work was supported in part by São Paulo Research Foundation (FAPESP), São Paulo, Brazil, under Grant 2014-24287-0, and in part by Programa CSF-PAJT, Brazil, under Grant 88887.064092-2014-00. Paper no. TPWRS-01616-2015.

J. López is with the Faculty of Engineering, School of Electrical Engineering, University of Cuenca, Cuenca 010150, Ecuador (e-mail: julio.lopez@ucuenca.edu.ec).

D. Pozo is with the Department of Electrical Engineering, Pontifical Catholic University of Rio de Janeiro, Rio de Janeiro 22430-060, Brazil (e-mail: davidpozocamara@gmail.com).

J. Contreras is with Escuela Técnica Superior de Ingenieros Industriales, Universidad de Castilla–La Mancha, Ciudad Real 13071, Spain (e-mail: Javier.Contreras@uclm.es).

J. R. S. Mantovani is with the Electric Power Systems Planning Laboratory, Department of Electrical Engineering, São Paulo State University, São Paulo 18618-000, Brazil (e-mail: mant@dee.feis.unesp.br).

Color versions of one or more of the figures in this paper are available online at http://ieeexplore.ieee.org.

Digital Object Identifier 10.1109/TPWRS.2016.2613544

$q_{G_{i,t}}$ Reactive power produced by generation unit in bus i and period t.

$qsh_{i,t}$ Reactive power produced by existing reactive power sources in bus i and period t.

$u^{+}_{i,t}, u^{-}_{i,t}$ Binary decision variables are equal to 1 if candidate reactive power source is installed in bus i and period t, and 0 otherwise.

Second-Stage Variables

$d_{i,t}(\omega)$ Auxiliary variable related with the convex formulation of the AC power flow equations in bus i, in period t and scenario ω.

$e_{\mathrm{ij,t}}(\omega), f_{\mathrm{ij,t}}(\omega)$ Variables from quadratic constraints associated with branch ij, in period t and scenario ω.

$p^{\mathrm{inj}}_{i,t}(\omega), q^{\mathrm{inj}}_{i,t}(\omega)$ Active and reactive power injections in bus i, in period t and scenario ω.

$p_{\mathrm{ij,t}}(\omega), q_{\mathrm{ij,t}}(\omega)$ Active and reactive power flow through transmission line ij, in period t and scenario ω.

$q^{+}_{i,t}(\omega), q^{-}_{i,t}(\omega)$ Capacitive and inductive reactive power dispatch of new reactive power source installed in bus i, in period t and scenario ω.

$t_{N_{\mathrm{ij,t}}}(\omega), t_{S_{\mathrm{ij,t}}}(\omega)$ Tap position and tap setting of tap-changing transformer in branch ij, in period t and scenario ω.

$v_{i,t}(\omega), \delta_{i,t}(\omega)$ Voltage magnitude and angle in bus i, in period t and scenario ω.

$l^{\mathrm{PI}}_{S_t}(\omega)$ Minimum load shedding computed from the perfect information problem for each period t and scenario ω.

$l_{S_{i,t}}(\omega)$ % of load shedding in bus i, in period t and scenario ω.

Functions

$\boldsymbol{\Phi}(\mathbf{t})$ Fixed costs function of candidate reactive power sources in period t.

$\boldsymbol{\Theta}(\mathbf{t},\omega)$ Operating costs function of candidate reactive power source in period t and scenario ω.

$\boldsymbol{\Gamma}(\mathbf{t},\omega)$ Difference function between the load shedding costs evaluated at the stochastic and perfect information optimization problems in period t and scenario ω.

$f(\cdot)$ Function of any specified input $(\cdot)$.

I. Introduction

Voltage collapse is generally associated with inadequate VAr support in power systems [1]. The limitations on production and transmission of reactive power lead to a deficit of reactive power. The focus of the VAr planning problem has been to determine the sizes and locations of shunt VAr sources and their efficient coordination with existing VAr sources to provide voltage support under normal system operating and contingency conditions [2]. Voltage collapse mostly occurs in heavily stressed power systems. It is usually associated with reactive power demands not being met because of limitations on production and transmission of reactive power. Sufficient reactive power support needs to be provided to maintain the power flow in transmission lines and buses within acceptable limits [3]. Then, VAr planning plays a very important role in improving power system reliability and security. It can be divided into two main parts: i) a planning sub-problem where decisions about the location and size of shunt VAr sources are made, and ii) operation sub-problem where VAr sources are scheduled to optimize system operation [4].

Planning and operating power systems is subject to a large degree of uncertainty due to the uncertainties in demand, availability of generation units, reliability of power system components, environmental regulation, and weather conditions [5]. Because forecasts can not be made exactly, decision makers use to considers such uncertainty. Uncertainty on the long-term decisions have higher impact in case of a low likelihood scenario realizes. Decision makers should include risk aversion in the decision making process to mitigate those potentially catastrophic scenario. Therefore, risk measure to account for those cases should optimize with total system expansion and operation costs resulting into a multi-objective optimization problem [6].

Most VAr planning problems have been traditionally solved as deterministic problems through successive linear and quadratic programming [7], nonlinear programming [8], [9], metaheuristic and hybrid techniques considering multiple objectives [10]–[13]. The deterministic problem considering security analysis has also been solved in [1], [14]. VAr planning problems considering uncertainty have not been widely addressed. In [15], VAr planning problem has been modeled using a chance constraint programming and solved by Monte Carlo Simulation with genetic algorithms. In [16] a long-term VAr planning problem has been solved considering demand uncertainty and contingency analysis. In [17] a novel approach for long-term reactive power planning using a mixed-integer stochastic convex model is proposed, where the risk of not meeting the load with a certain level of confidence due to a reactive power deficit is represented by chance constraints. In [18], [19] the VAr planning problem containing multiple objectives (system investment, system operational efficiency, system security, system service quality and voltage deviation of the system) is solved using the ϵ-constraint method based firstly on the classical and extended simulated annealing approach.

Previous literature shows that the majority of the current VAr planning problems have been set considering deterministic approaches with a single objective function without taking into account any sources of uncertainty affecting the power system. Ignoring uncertainty produces erroneous or unrealistic solutions, resulting in inadequate VAr support. The solution of optimization problems with only one objective function (generally based on expected cost minimization) is straightforward because the output is a single optimal solution. For example, a non-linear mixed integer VAr planning model is proposed in [16], where risk analysis and the discretization of transformer tap settings are ignored.

As a consequence, power systems are being operated close to their maximum power transfer capability limits, making the system more vulnerable to voltage instability events.

Recently, new convex AC optimal power flow models have been proposed. In [20], the transmission network expansion problem is solved by means of conic optimization, in [21] the optimal power flow is solved using semidefinite programming. However, none of these types of convex power flow equation have been used to solve the reactive planning problem yet. Our proposed model extends the AC conic optimization power flow approach [20] for solving the VAr planning problem considering tap changing transformers and stochastic demand.

Robust optimization has been applied in many unit commitment and transmission network expansion problems, but not in VAr planning problems. In [22] two robust optimization models, minimax cost and minimax regret-based are addressed to solve the transmission expansion planning problem, considering load and generation uncertainties. In [23], the unit commitment problem considering an $n-K$ security criterion problem is solved using bilevel programming, which is solved by transforming the bilevel problem to an equivalent single-level problem. In [24], a two-stage robust unit commitment model is proposed considering wind output uncertainty, with the objective of providing a robust schedule for the thermal generators in the day-ahead market that minimizes the total cost under the worst wind power output scenario. To overcome the robust optimization conservativeness, [25] proposes a tradeoff between the security-constrained unit commitment cost and the recourse cost requirement related with reserves needs. In [26], a two-stage adaptive robust unit commitment model considering security constrained and nodal net injection uncertainty is proposed, where Benders' decomposition is used to solve the problem. A minimax regret approach is proposed in [27] for the unit commitment problem solution considering wind power generation uncertainty, where Benders' decomposition is used to solve the problem.

A. Aims and Contributions

In this paper we propose a risk-based methodology to deal with the long-term VAr planning problem under uncertainty. The main contributions of this paper are as follows:

1) The proposed risk-based model for the VAr planning problem consists of a multi-period and multi-objective two-stage stochastic mixed integer quadratically-constrained formulation that guarantees optimum global solutions and allows for trade-offs between investment costs and load shedding risk.
2) Instead of using average fixed values for the demands, scenarios are generated to model demand uncertainties in each period along the planning horizon.
3) The proposed problem integrates power system reliability enhancement by means of the min-max regret paradigm, reducing load shedding in the worst scenarios.
4) VAr sources are allocated and reactive power dispatching decisions are carried out while reducing investment costs and load shedding risk with a limited range of possible expansion plans.
5) Tap-changing transformers are important for reactive power/voltage magnitude control. In the proposed VAr planning formulation the modeling of the tap-changing transformers is done via discrete variables for the sake of accuracy and a convex AC power flow model is used.

All this contributes to increasing the accuracy of the formulation while transforming the problem into a mixed integer one. The problem is constructed so that a reliable VAr planning can be achieved. The proposed multi-period planning is simultaneously optimized for the entire time horizon where unknown variables for the whole problem are determined.

The remaining sections are outlined as follows. Section II describes the main characteristics of the proposed decision framework. Section III presents the mathematical formulation of the problem. Section IV depicts the solution approach to solve the problem. Section V the analyzes and discusses results from a case study. Finally conclusions are drawn in Section VI.

II. Modeling Framework

A. Risk Modeling

Risk modeling is incorporated in the proposed problem by means of min-max regret optimization [22], [28]. The regret measures the distance between the load shedding cost of the actual stochastic optimal solution and the load shedding cost considering perfect information, i.e., if the VAr planning problem were solved for a single scenario.

The regret, $\Gamma(t,\omega)$, is formulated in (1).

$$\Gamma(t,\omega) = CLS(t,\omega) - CLS^{\mathrm{PI}}(t,\omega), \quad \forall t, \forall \omega \tag{1}$$

The first term represents the cost of load shedding in all $\mathcal{PQ}$ buses evaluated at the stochastic problem optimal solution, $CLS^{\mathrm{PI}}(t,\omega)$. The second term represents the minimum cost of load shedding if the VAr planning problem were solved with perfect information (PI), $CLS^{\mathrm{PI}}(t,\omega)$. Observe that $CLS^{\mathrm{PI}}(t,\omega)$ is calculated ex-ante in our model.

The maximum regret (2) is used here as a risk measure. It is minimized in the multi-objective VAr planning problem avoiding regrets resulting from making a risky decision. Therefore, the VAr expansions that have serious consequences in any of the considered scenarios will be not be chosen. It evaluates the worst-case regret for all possible load scenarios in each period along the planning horizon. Therefore, the decision maker looks for a solution which will give a level of satisfaction as close as possible to the optimal situation (which can only be known a posteriori), whatever situation occurs in the future.

$$\Gamma^{\max}(t) = \max_{\omega\in\mathbf{\Omega}} \Gamma(t,\omega) \tag{2}$$

B. Multi-Objective Model

In a multi-objective optimization models decisions are optimized according to two or more conflicting criteria. In this paper, the proposed multi-objective problem has two conflicting objectives: i) minimization of the current value of the fixed and expected operating costs of new VAr sources installed along the planning horizon, $f_1(\cdot)$, and ii) minimization of the risk associated with load shedding due to the reactive power deficit associated to demand uncertainty, $f_2(\cdot)$. Minimizing only the economic objective function (fixed and expected operating costs) can result in large load shedding (degrading the security).

A popular way in the literature of multi-objective optimization is to consider Pareto optimal solutions.

In a Pareto solution or non-inferior solution any improvement of one objective function can be achieved only at the expense of degrading the others. The set of solutions composes the trade-off set known as a Pareto efficient frontier.

The multi-objective optimization problem is stated as (3),

$$\min \mathbf{F}\left\{f_1(\mathbf{\Phi}(t), \mathbf{\Theta}(t,\omega)), f_2(\Gamma^{\max}(t))\right\} \tag{3}$$

where $\mathbf{\Phi}(t)$ represents the VAr investment costs in period t, $\mathbf{\Theta}(t,\omega)$ represents the operating costs of the VAr sources dispatching decision in period t and scenario ω, and $\Gamma^{\max}(t)$ represents the maximum regret in period t.

C. Load Shedding in an AC Convex Power Flow

Load shedding occurs in emergency conditions when the load can not be met because of a reactive power deficit in any scenario along the planning horizon. One method that considers only one load shedding factor was proposed in [29]. Considering the demand power factor constant, we can associate variable $l_{S_{i,t}}(\omega)$ with the forecasted active and reactive loads, $P_{D\,i,t}(\omega)$ and $Q_{D\,i,t}(\omega)$, respectively, as follows:

$$P_{D\,i,t}(\omega)(1 - l_{S_{i,t}}(\omega)) \quad \forall i \in \mathcal{PQ},\ \forall t \in \mathcal{P},\ \forall \omega \in \Omega \tag{4}$$

$$Q_{D\,i,t}(\omega)(1 - l_{S_{i,t}}(\omega)) \quad \forall i \in \mathcal{PQ},\ \forall t \in \mathcal{P},\ \forall \omega \in \Omega \tag{5}$$

$$0 \leq l_{S_{i,t}}(\omega) \leq 1 \quad \forall i \in \mathcal{PQ},\ \forall t \in \mathcal{P},\ \forall \omega \in \Omega \tag{6}$$

where $l_{S_{i,t}}(\omega)$ is expressed in %, if $l_{S_{i,t}}(\omega) = 0$ there is no load shedding, and if $l_{S_{i,t}}(\omega) = 1$ the total load is shed.

In the proposed VAr planning problem the nonlinear equations of the AC active and reactive power flow injections are represented as a set of convex equations. Hence, the formulation presented in [20] is extended to a set of linear and quadratic constraints for the long-term stochastic AC active and reactive power flow injections. With that reformulation, the proposed VAr planning problem becomes a convex quadratically-constrained problem that guarantees a global optimal solution.

To guarantee the solvability of the optimization problem when the load can not be met in any scenario along the planning horizon, new variables representing the synchronous compensator reactive power dispatches and load shedding must be inserted at the reformulated convex quadratically-constrained long-term stochastic power balance equations, as follows:

$$P_{G\,i,t} + p^{\mathrm{sl}}_{G_{i,t}} - P_{D\,i,t}(\omega)(1 - l_{S_{i,t}}(\omega)) - p^{\mathrm{inj}}_{i,t}(\omega) = 0 \tag{7}$$

$$q_{G\,i,t} - Q_{D\,i,t}(\omega)(1 - l_{S_{i,t}}(\omega)) + qsh_{i,t} + q^{+}_{i,t}(\omega) - q^{-}_{i,t}(\omega) - q^{\mathrm{inj}}_{i,t}(\omega) = 0 \tag{8}$$

$$d_{i,t}(\omega) d_{j,t}(\omega) \geq e^2_{\mathrm{ij,t}}(\omega) + f^2_{\mathrm{ij,,t}}(\omega) \tag{9}$$

$$-\epsilon_\delta \leq \delta_{i,t}(\omega) - \delta_{j,t}(\omega) - f_{\mathrm{ij,t}}(\omega) \leq \epsilon_\delta \tag{10}$$

$$e_{\mathrm{ij,t}}(\omega) \geq 0 \tag{11}$$

$$\forall i \in \mathcal{N},\ \forall ij \in \mathcal{L} \cup \mathcal{T},\ \forall t \in \mathcal{P},\ \forall \omega \in \Omega$$

where (7) and (8) are the AC active and reactive power balance equations,[1] respectively. Quadratic equations (9) and (10) come from the reformulation of the nonlinear equations of the AC active and reactive power injections.

D. Tap-Changing Transformers

Regarding the tap-changing transformers, the proposed formulation includes discrete tap-changing transformers. In these devices, the tap is adjusted in the primary or secondary winding by a tap changer mechanism, which is categorized by a regulation range (R_{ij}) and a set of steps (connection points) along the winding (S_{ij}). R_{ij} and S_{ij} are known parameters, e.g., $\pm 10\%$, 32 steps. The proposed discrete formulation is made considering the continuous tap-changing transformer formulation [31] in (12).

$$(T^{\min}_{\mathrm{ij}})^2 d_{j,t}(\omega) \leq d_{i,t}(\omega) \leq (T^{\max}_{\mathrm{ij}})^2 d_{j,t}(\omega) \quad \forall ij \in \mathcal{T},\ \forall t \in \mathcal{P},\ \forall \omega \in \Omega \tag{12}$$

From (12), $T^{\min}_{\mathrm{ij}} = 1 - R_{\mathrm{ij}}$. We can formulate a expression that computes $d_{j,t}(\omega)$ by setting discrete $t_{N_{\mathrm{ij}}}(\omega)$ as in (13), which is limited by the upper and lower steps (14).

$$d_{j,t}(\omega) = (T^{\min}_{\mathrm{ij}})^2 d_{i,t}(\omega) + \frac{4R_{\mathrm{ij}}}{S_{\mathrm{ij}}} t_{N_{\mathrm{ij}}}(\omega) d_{i,t}(\omega) \quad \forall ij \in \mathcal{T},\ \forall t \in \mathcal{P},\ \forall \omega \in \Omega \tag{13}$$

$$-\frac{S_{\mathrm{ij}}}{2} \leq t_{N_{\mathrm{ij}}}(\omega) \leq \frac{S_{\mathrm{ij}}}{2} \quad \forall ij \in \mathcal{T},\ \forall t \in \mathcal{P},\ \forall \omega \in \Omega \tag{14}$$

$$t_{N_{\mathrm{ij}}}(\omega) \in \mathcal{Z} \quad \forall ij \in \mathcal{T},\ \forall t \in \mathcal{P},\ \forall \omega \in \Omega \tag{15}$$

The mixed integer nonlinear expressions, (13)–(15), can be reformulated to a set of mixed integer linear equations. Integer variable $t_{N_{\mathrm{ij}}}(\omega)$ can be described by means of binary variables using a binary expansion [32], as shown in (16)–(18).

$$t_{N_{\mathrm{ij}}}(\omega) = \sum_{\substack{m \in \mathcal{M} \\ m=1}}^{[\log_2(NS_m)]} 2^{(m-1)} x_{\mathrm{ij,m,t}}(\omega) - \frac{S_{\mathrm{ij}}}{2} \quad \forall ij \in \mathcal{T},\ \forall t \in \mathcal{P},\ \forall \omega \in \Omega \tag{16}$$

$$t_{N_{\mathrm{ij,t}}}(\omega) \in \mathcal{Z} \quad \forall ij \in \mathcal{T},\ \forall t \in \mathcal{P},\ \forall \omega \in \Omega \tag{17}$$

$$x_{\mathrm{ij,m,t}}(\omega) \in \{0,1\} \quad \forall ij \in \mathcal{T},\ \forall t \in \mathcal{P},\ \forall \omega \in \Omega \tag{18}$$

By replacing (16)–(18) in (13)–(15), a mixed binary nonlinear product is obtained $x_{\mathrm{ij,m,t}}(\omega) d_{i,t}(\omega)$, which can be reformulated to linear constraints similar to the methodology used [32] by means of big-M approach. We replace this non-linear product by an auxiliary variable, $y_{\mathrm{ij,m,t}}(\omega)$, and its linearization

[1] Note that the active power output of the generators, $P_{G\,i,t}$, is already known as in current VAr planning approaches. See [14], [30] for further details.

is obtained adding constraints (19)–(24).

$$d_{j,t}(\omega)=(1-R_{\mathrm{ij}})^2 d_{i,t}(\omega)+\frac{4R_{\mathrm{ij}}}{S_{\mathrm{ij}}}\sum_{\substack{m\in\mathcal{M}\\ m=1}}^{[\log_2(S_{\mathrm{ij}})]} 2^{(h-1)} y_{\mathrm{ij,m,t}}(\omega)$$
$$\forall ij\in\mathcal{T},\ \forall t\in\mathcal{P},\ \forall\omega\in\Omega \quad (19)$$

$$y_{\mathrm{ij,m,t}}(\omega)\ge\frac{\left[(1-R_{\mathrm{ij}})V_i^{\min}\right]^2}{\sqrt{2}}x_{\mathrm{ij,m,t}}(\omega)$$
$$\forall ij\in\mathcal{T},\ \forall t\in\mathcal{P},\ \forall\omega\in\Omega \quad (20)$$

$$y_{\mathrm{ij,m,t}}(\omega)\le\frac{\left[(1+R_{\mathrm{ij}})V_i^{\max}\right]^2}{\sqrt{2}}x_{\mathrm{ij,m,t}}(\omega)$$
$$\forall ij\in\mathcal{T},\ \forall t\in\mathcal{P},\ \forall\omega\in\Omega \quad (21)$$

$$d_{i,t}(\omega)-y_{\mathrm{ij,m,t}}(\omega)\ge\frac{\left[(1-R_{\mathrm{ij}})V_i^{\min}\right]^2}{\sqrt{2}}\left[1-x_{\mathrm{ij,m,t}}(\omega)\right]$$
$$\forall ij\in\mathcal{T},\ \forall t\in\mathcal{P},\ \forall\omega\in\Omega \quad (22)$$

$$d_{i,t}(\omega)-y_{\mathrm{ij,m,t}}(\omega)\le\frac{\left[(1+R_{\mathrm{ij}})V_i^{\max}\right]^2}{\sqrt{2}}\left[1-x_{\mathrm{ij,m,t}}(\omega)\right]$$
$$\forall ij\in\mathcal{T},\ \forall t\in\mathcal{P},\ \forall\omega\in\Omega \quad (23)$$

$$x_{\mathrm{ij,m,t}}(\omega)\in\{0,1\}\ \ \forall ij\in\mathcal{T},\ \forall t\in\mathcal{P},\ \forall\omega\in\Omega \quad (24)$$

III. The VAr Planning Model

The proposed VAr planning problem expressed in a compact form is represented as follows:

$$\min_{\mathbf{z(t},\omega)} \mathbf{F}\left\{f_1(\cdot),f_2(\cdot)\right\} \quad (25)$$

s.t.:

$$\mathbf{C}^{\mathrm{inv}}(\mathbf{z(t)})\le\mathbf{B} \quad (26)$$
$$\mathbf{\Gamma}^{\max}(\mathbf{t})=\max_{\omega\in\mathbf{\Omega}}\mathbf{\Gamma}(\mathbf{z}(\mathbf{t},\omega)) \quad (27)$$
$$\mathbf{G}(\mathbf{x}(\mathbf{t},\omega),\mathbf{z}(\mathbf{t},\omega))=\mathbf{0} \quad (28)$$
$$\mathbf{x}^{\min}\le\mathbf{x}(\mathbf{t},\omega)\le\mathbf{x}^{\max} \quad (29)$$
$$\mathbf{z}^{\min}\le\mathbf{z}(\mathbf{t},\omega)\le\mathbf{z}^{\max} \quad (30)$$
$$\mathbf{z_I}(\mathbf{t},\omega)\in\mathbf{Z} \quad (31)$$
$$\mathbf{z_b}(\mathbf{t},\omega)\in\{\mathbf{0/1}\} \quad (32)$$

where (25) represents the multi-objective set of functions to be simultaneously minimized represented by (33) and (34).

$$f_1(\cdot)=\sum_{t\in\mathcal{P}|t=1}\frac{1}{(1+I_t)^t}\left\{\sum_{i\in\mathcal{K}}C_i^{\mathrm{fix}}\left(u_{i,t}^{+}+u_{i,t}^{-}\right)\right.$$
$$\left.+\,\mathbb{E}\left[\sum_{i\in\mathcal{K}}C_i^{\mathrm{op}}\left(q_{i,t}^{+}(\omega)+q_{i,t}^{-}(\omega)\right)\right]\right\}$$
$$\sum_{t\in\mathcal{P}|t>1}\frac{1}{(1+I_t)^t}\left\{\sum_{i\in\mathcal{K}}C_i^{\mathrm{fix}}\left[(u_{i,t}^{+}-u_{i,t-1}^{+})+(u_{i,t}^{-}-u_{i,t-1}^{-})\right]\right.$$
$$\left.+\,\mathbb{E}\left[\sum_{i\in\mathcal{K}}C_i^{\mathrm{op}}\left(q_{i,t}^{+}(\omega)+q_{i,t}^{-}(\omega)\right)\right]\right\} \quad (33)$$

$$f_2(\cdot)=\sum_{t\in\mathcal{P}}\frac{1}{(1+I_t)^t}\Gamma_t^{\max} \quad (34)$$

Constraint (26) represents the expansion budget stated by (35).

$$\sum_{t\in\mathcal{P}|t=1}\frac{1}{(1+I_t)^t}\left[C_i^{\mathrm{fix}}\left(u_{i,t}^{+}+u_{i,t}^{-}\right)\right]+\sum_{t\in\mathcal{P}|t>1}\frac{1}{(1+I_t)^t}$$
$$\left\{C_i^{\mathrm{fix}}\left[(u_{i,t}^{+}-u_{i,t-1}^{+})+(u_{i,t}^{-}-u_{i,t-1}^{-})\right]\right\}\le B\ \forall i\in\mathcal{K} \quad (35)$$

The maximum regret definition (27), can be replaced by a set of inequalities (36) where the $\Gamma_t^{\max}$ is an upper bound of the regret function in any scenario ω.

$$\Gamma_t^{\max}\ge\Gamma(t,\omega)\ \forall t\in\mathcal{P},\ \forall\omega\in\Omega \quad (36)$$

Equation (28) represents the linear and quadratic equation set of AC active and reactive power balance (7)–(11) equations. Constraints (29) and (30) represent the lower and upper limits of state and control variables (19)–(23), (37)–(42), and (47), respectively. The integer and binary variables in (31) and (32) represent the tap-changing transformers and the decision to install VAr sources, (24) and (43)–(46), respectively.

$$Q_{G_i}^{\min}\le q_{G\,i,t}\le Q_{G_i}^{\max}\quad\forall i\in\mathcal{G},\ \forall t\in\mathcal{P},\ \forall\omega\in\Omega \quad (37)$$

$$(V_i^{\min})^2\le d_{i,t}(\omega)\le(V_i^{\max})^2$$
$$\forall i\in\mathcal{N},\ \forall t\in\mathcal{P},\ \forall\omega\in\Omega \quad (38)$$

$$p_{\mathrm{ij},t}^2(\omega)+q_{\mathrm{ij},t}^2(\omega)\le(S_{\mathrm{ij}}^{\max})^2$$
$$\forall ij\in\mathcal{L},\ \forall t\in\mathcal{P},\ \forall\omega\in\Omega \quad (39)$$

$$Q_{\mathrm{SH_i}}^{\min}\le qsh_{i,t}\le Q_{\mathrm{SH_i}}^{\max}\ \ \forall i\in\mathcal{E},\ \forall t\in\mathcal{P}\in\Omega \quad (40)$$

$$q_{i,t}^{+}(\omega)\le Q_{P_i}^{\max}u_{i,t}^{+}\qquad\forall i\in\mathcal{K},\ \forall t\in\mathcal{P},\ \forall\omega\in\Omega \quad (41)$$

$$q_{i,t}^{-}(\omega)\le Q_{N_i}^{\max}u_{i,t}^{-}\qquad\forall i\in\mathcal{K},\ \forall t\in\mathcal{P},\ \forall\omega\in\Omega \quad (42)$$

$$u_{i,t}^{+}+u_{i,t}^{-}\le 1\qquad\forall i\in\mathcal{K},\ \forall t\in\mathcal{P} \quad (43)$$

$$u_{i,t}^{+}\le u_{i,t-1}^{+}\qquad\forall i\in\mathcal{K},\ \forall t\in\mathcal{P} \quad (44)$$

$$u_{i,t}^{-}\le u_{i,t-1}^{-}\qquad\forall i\in\mathcal{K},\ \forall t\in\mathcal{P} \quad (45)$$

$$\{u_{i,t}^{+},u_{i,t}^{-}\}\in\{0,1\} \quad (46)$$

$$\left\{d_{i,t}(\omega),q_{i,t}^{+}(\omega),q_{i,t}^{-}(\omega)\right\}\ge 0 \quad (47)$$

IV. Epsilon-Based Solution Approach

The ϵ-constraint method [33] is, along with the weighting method, one of the two most popular methods for solving multi-objective problems.

As described in [34], the ϵ-constraint method has certain advantages in relation to the weighting method, especially in the presence of integer decision variables, as in our problem.

To build the efficient set, one of the objective functions is optimized using the other objective functions as constraints. The generated constraints limits the value of the other objective functions and they are accordingly updated in each iteration. Hence, for our proposed problem, the ϵ-constraint method would minimize the investment and expected operation cost while limiting the risk of having load shedding (48). The load shedding risk bound is updated in each iteration as in (49). $f_2^{\max}$ and $f_2^{\min}$ represent the maximum and minimum values of the individual objective function based on the payoff table [33], respectively.

$$\min f_1\big(\mathbf{\Phi}(t), \mathbf{\Theta}(t,\omega)\big) \tag{48}$$

$$\text{s.t. : } \begin{cases} f_2(\Gamma^{\max}(t,\omega)) \le \epsilon_{2,s} \\ \text{All constraints represented by (26)–(32)} \end{cases}$$

where

$$\epsilon_{2,s} = f_2^{\max} - \left[\frac{f_2^{\max} - f_2^{\min}}{L_2}\right] \times s$$
$$s = 0, 1, 2 \ldots, L_2 \tag{49}$$

The range of the second objective function, $f_2(\Gamma^{\max}(t,\omega))$, is divided into L_2 equal intervals using $(L_2 - 1)$ intermediate equidistant grid points. Considering the minimum and maximum values of the range, there is a total $(L_2 + 1)$ grid points for $f_2(\cdot)$. Hence, $(L_2 + 1)$ optimization subproblems have to be solved where some of these optimization subproblems may have an infeasible solution space, which will be discarded. Practically, the case of infeasibilities is disregarded using the early exit from the nested loops. Note that by solving each optimization problem, a single Pareto optimal solution is obtained. Sequentially, the Pareto efficient frontier is constructed. After obtaining the Pareto optimal solutions by solving the optimization subproblems, the decision maker should choose the best compromise solution according to its specific preference among all Pareto optimal solutions.

V. Case Study

A. Data Specifications

To illustrate the efficient performance of the proposed methodology, numerical results are presented for the real equivalent South and South-East Brazilian Power System [35], it is comprised of two areas: 230 kV South Brazil area and 500 kV South-East Brazil area. The system comprises 65 buses, 14 generating units, 51 load buses, 1 continuous reactive power source, 6 switched shunt capacitor banks, 3 not switched shunt capacitor banks, 6 switched shunt inductor banks, 8 not switched shunt inductor banks, 25 fixed tap transformers, 18 load tap changing transformers and 53 transmission lines.

Load forecast uncertainty at all $\mathcal{PQ}$ buses over the planning horizon is introduced into the problem by means of a Normal distribution function, $N(\mu_t, \sigma_t)$, (with an average value, μ and a standard deviation, σ) for every time period $t \in T$. Monte Carlo simulation is used to generate load scenarios with known probability $\pi(\omega)$ for each year. To better capture the tails of the normal distribution (generally associated with the risk scenarios), a Latin Hypercube sampling technique [36] is used.

TABLE I
Capacity and Costs of Candidate VAr Power Sources

BUS	$Q_{P_i}^{\max}$ [MVAr]	$Q_{N_i}^{\max}$ [MVAr]	C_i^{fix} [10^6 US$]	C_i^{op} [US$/MVAr]
18–213	300	300	60	120.87
217–536	500	500	100	95.83
814–897	100	100	20	192.00
898–965	400	400	80	102.58
976–2458	200	200	40	150.69

The additional following considerations have been made:

1) The planning horizon is four years divided into periods of one year for each t. Each period has 52 load scenarios, and each scenario corresponds to a weekday sample, with same probability and 15% of standard deviation.
2) A 7% annual interest rate is utilized to calculate the present value of the investment throughout the planning horizon [16].
3) All buses are considered as candidate buses to install continuous reactive power sources.
4) Load scenarios in each stage are generated assuming 3% annual expected load growth rate.
5) The upper and lower voltage magnitude limits in all buses are $[0.95-1.05]$ p.u.
6) To the tap-changing transformers, the regulating transformer and the number of steps are 10% and 32 steps (± 16), respectively.
7) The cost of $C_{i,t}^{\text{ls}}$ of load shedding for each $\mathcal{PQ}$ bus is $50.00.

For the simulations, we consider continuous reactive power sources with three different capacities distributed along all the buses. Table I presents the fixed and operating costs data for the new capacitive and inductive reactive power source candidates to be installed. The investment budget is limited to the fixed cost of each reactive power source, the expansion planning costs containing the fixed plus the operating costs.

B. Results

The proposed methodology has been carried out using the optimization solver CPLEX 12.6 [37] in AMPL [38], in a Dell PowerEdge R910x64, 128 GB of RAM and 1.87 GHz. The average computational time required to achieve the optimal solutions for all the simulations has been 128.18 min. Table II lists the expansion cost for installing new reactive capacitive power sources, the load shed, the risk measure, and the corresponding RPP attained from solving the risk neutral and risk averse problems for different expansion budgets.

We can see that the risk averse solutions propose higher expansion costs and lower risk levels compared with the risk neutral solutions. Regarding the expansion costs increments represent 11.25%, 11.23%, 7.92% and 6.28% for investment budgets of US$20 million, US$40 million, US$60 million and US$80 million, respectively. For budgets ranging from US$100 million to US$400 million, the expansion costs are the same. Regarding the risk levels costs reductions represent 59.51%, 43.29%,

TABLE II
RISK-NEUTRAL VS. RISK-AVERSE SOLUTIONS

Risk-Neutral Solutions								
B	Expansion Cost	Expected Load Shed		Risk	Expansion Plan			
[10^6 US$]	[10^6 US$]	P [MW]	Q [MVAr]	[10^3 US$]	T_1	T_2	T_3	T_4
20	18.86	1594.72	1012.12	35.37	840	-	-	-
40	37.71	1310.02	869.10	21.71	834, 840	-	-	-
60	56.50	1066.35	673.21	13.60	840, 1210	-	-	-
80	74.09	799.12	519.31	5.52	834, 1210	840	-	-
100	92.71	702.30	309.10	4.37	956	840	-	-
200	186.70	261.22	88.87	1.95	123, 814, 834, 965	840	-	-
400	368.80	0.00	0.00	0.00	102, 123, 834, 840, 960, 964, 1210	-	-	976
Risk-Averse Solutions								
B	Expansion Cost	Expected Load Shed		Risk	Expansion Plan			
[10^6 US$]	[10^6 US$]	P [MW]	Q [MVAr]	[10^3 US$]	T_1	T_2	T_3	T_4
20	21.25	1581.57	1006.42	14.32	840	-	-	-
40	42.03	1304.33	863.15	12.31	834, 839	-	-	-
60	61.36	1057.28	668.65	9.34	840, 976	-	-	-
80	79.06	791.98	515.34	4.36	834, 840, 976	-	-	-
100	92.72	695.35	302.42	3.92	965	839	-	-
200	186.73	250.83	83.65	1.78	123, 814, 834, 965	840	-	-
400	368.82	0.00	0.00	0.00	102, 123, 834, 840, 848, 965, 976, 1015, 1210	-	-	-

TABLE III
EFFICIENT FRONTIER FOR TWO EXPANSION BUDGETS

Budget = $80 Million							
Risk	Expansion Cost	Expected Load Shed		Expansion Plan			
[10^3 US$]	[10^6 US$]	P [MW]	Q [MVAr]	T_1	T_2	T_3	T_4
14.32	18.86	1594.72	1012.12	840	-	-	-
12.20	24.02	1402.13	972.52	840	-	-	-
9.33	33.70	1380.15	889.12	840, 976	-	-	-
7.21	45.03	1102.08	678.14	839	840	-	-
5.51	60.50	1066.35	673.21	840	976	-	-
4.66	75.35	854.13	812.14	834, 976	840	-	-
Budget = $100 Million							
Risk	Expansion Cost	Expected Load Shed		Expansion Plan			
[10^3 US$]	[10^6 US$]	P [MW]	Q [MVAr]	T_1	T_2	T_3	T_4
14.32	18.86	1594.72	1012.12	840	-	-	-
12.20	24.02	1402.13	972.52	840	-	-	-
9.33	37.71	1310.02	869.10	840, 976	-	-	-
6.51	56.50	1066.35	673.21	834, 839	-	-	-
4.66	74.09	799.12	519.31	834, 976	840	-	-
3.92	92.71	702.30	309.10	965	839	-	-

31.32%, 21.01%, 10.30% and 8.72% for investment budgets of US$20 million, US$40 million, US$60 million, US$80 million, US$100 million and US$200 million, respectively. On the other hand, the small differences in the load not served costs are due to the fact that the risk neutral and risk averse VAr planning problems are not identical.

Table III provides information about the risk and expansion cost tradeoff for $80 and $100 expansion budgets. We can see that, for each risk level ($RL_{1,s}$), total load shedding (P, Q) and expansion costs for the newly allocated reactive power sources are obtained. The expansion plan is shown for each period and the buses where reactive power sources are installed. This is very important for the transmission system planner because it provides relevant information on the trade-off between risk mitigation and incurred expansion costs in each expansion plan. These data correspond to the efficient frontier and they are helpful for selecting an appropriate expansion plan. The efficient frontier is composed of a few points because of the discrete nature of the problem. For example, if the transmission expansion planner is interested in a strictly risk-averse position (minimum load not served), ($RL_{1,0} = \$3.92 \times 10^3$) the maximum reactive capacitive power sources are installed in periods 1 and 2, resulting in the highest reactive expansion costs. In contrast, lower reactive expansion planning costs, result in higher load not served ($RL_{1,5} = \$14.32 \times 10^3$).

Fig. 1 plots the expected load shed in % for $100 million budget expansion in each period for the tradeoff risk levels. We can see as in each period the expected load shed is minimized from higher to lower risk. For example Fig. 1(a) shows that the maximum expected load shed is 13.16% in PQ-bus 965 for a risk of $14.32 $\times 10^3$ in stage $T = 1$. This implies expansion costs (fixed + operating) of $18.86 million for installing a newly reactive source in bus 840 in stage $T = 1$. Figs. 1(b), 1(c) and 1(d) show that PQ-bus 965 is subject to a greater expected load shed for a higher risk and other PQ-buses appear in the next stages because of demand growth where the load is shed as well.

Fig. 2 shows the box-plot for the reactive power dispatches in each stage of the newly installed reactive power source for a minimum regret ($RL_{1,0} = \$3.92 \times 10^3$) and $100 million expansion budget. The box-plot provides basic information about a distribution, the 25th and 75th quartiles are represented for the lower and upper corners respectively, the median value is represented by the horizontal line in the box, the square point in the box represents the mean value, the minimum and maximum values and the atypical values are shown as well. Fig. 2(a) shows

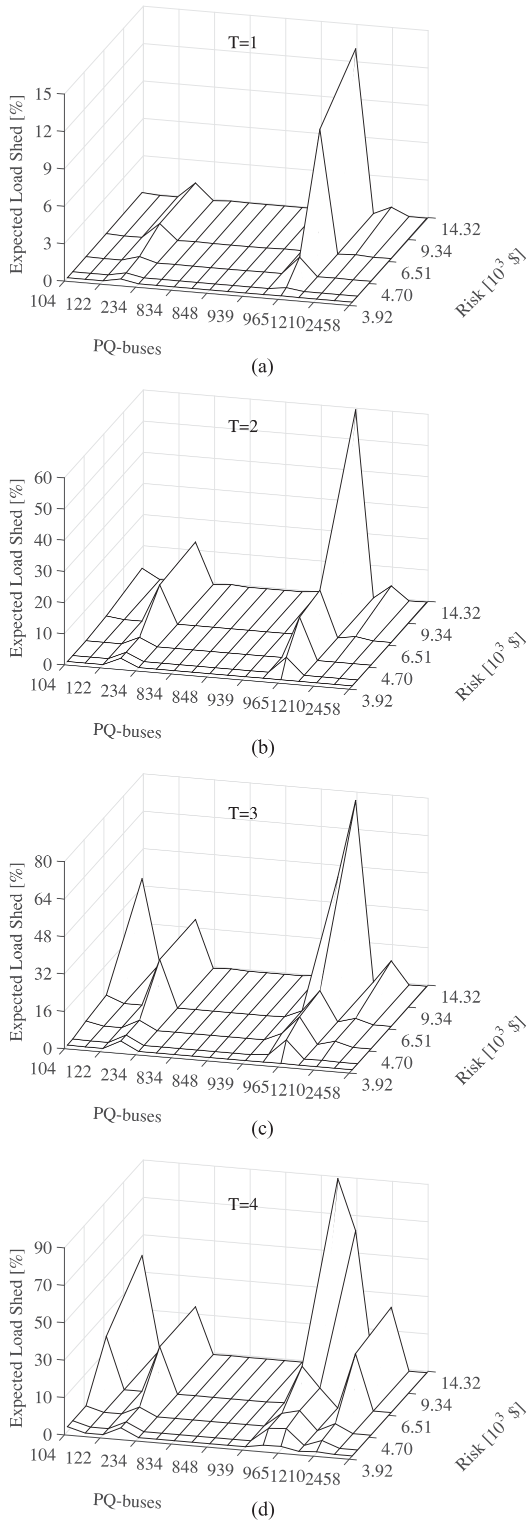

Fig. 1. Load not served for different regret levels and \$100 million expansion budget.

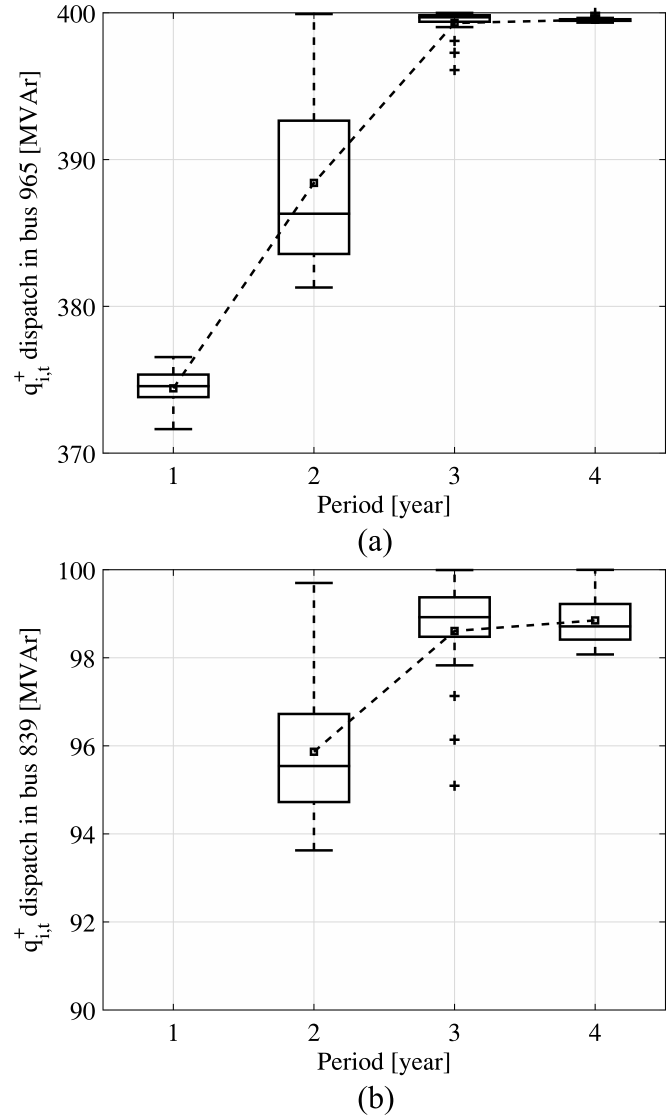

Fig. 2. Reactive power dispatch for minimum regret and \$100 million expansion budget.

the reactive power dispatch distribution function with means of 374.41 in T_1, 388.41 in T_2, 399.31 in T_3 and 399.53 in T_4 and medians of 374.56 in T_1, 386,31 in T_2, 399.69 in T_3 and 399.46 in T_4. Fig. 2(b) shows the reactive power dispatch distribution function beginning at stage T_2 with means of 95.87 in T_2, 98.61 in T_3 and 98.84 in T_4 and medians of 95.54 in T_2, 98.92 in T_3 and 98.71 in T_4.

Fig. 3 shows the box-plot for the reactive power dispatches in each stage of the newly installed reactive power source for a maximum regret ($RL_{1,5} = \$14.32 \times 10^3$) and \$100 million expansion budget. We can see that the reactive power dispatch distribution function has means of 94.26 in T_1, 95.73 in T_2, 98.62 in T_3 and 98.43 in T_4 and medians of 93.76 in T_1, 95.12 in T_2, 98.87 in T_3 and 98.24 in T_4.

In the proposed methodology the solutions for the tap settings of ULTC transformers are integer values representing the positions in the windings transformer. The solutions for the 18 ULTCs in 4 periods and 52 scenarios per period are difficult to show in the present format, therefore, the tap positions with their corresponding tap setting solutions for the risk-averse RPP problem for each period for the minimum, average and maximum demand scenarios are shown for each column of Table IV.

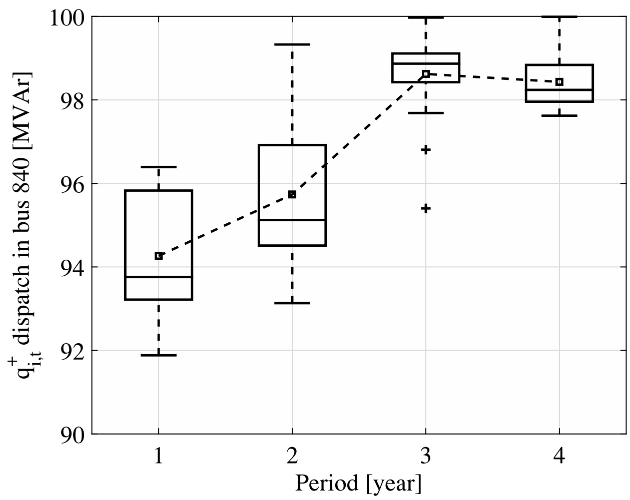

Fig. 3. Reactive power dispatch for maximum regret and $100 million expansion budget.

TABLE IV
TAP SETTINGS OF ULTCS FOR THE RISK-AVERSE APPROACH

Period	ULTCs by Branch	$\omega^{\min}_{(P_D,Q_D)}$ Pos.	Set	$\omega^{\text{average}}_{(P_D,Q_D)}$ Pos.	Set	$\omega^{\max}_{(P_D,Q_D)}$ Pos.	Set
	2x(814–895)	–3	0.9812	–3	0.9812	2	1.0125
	2x(839–840)	–1	0.9938	0	1.0000	4	1.0250
	898–848	0	1.0000	0	1.0000	0	1.0000
	934–933	–13	1.0884	–8	1.0526	0	1.0000
T = 1	3x(939–938)	–6	0.9625	–2	0.9875	0	1.0000
	2x(960–959)	–3	0.9812	0	1.0000	3	1.0188
	2x(965–964)	–9	0.9437	–5	0.9688	–2	0.9875
	3x(1210–976)	0	1.0000	0	1.0000	2	1.0125
	1503–1504	2	1.0125	2	1.0125	4	1.0250
	2458–896	–4	0.9750	–1	0.9938	3	1.0188
	2x(814–895)	–1	0.9938	–1	0.9938	6	1.0375
	2x(839–840)	2	1.0125	1	1.0063	9	1.0562
	898–848	4	1.0250	2	1.0125	8	1.0500
	934–933	–5	0.9688	–3	0.9812	1	1.0063
T = 2	3x(939–938)	–4	0.9750	–2	0.9875	1	1.0063
	2x(960–959)	–1	0.9938	1	1.0063	5	1.0313
	2x(965–964)	–7	0.9563	–3	0.9812	1	1.0063
	3x(1210–976)	1	1.0063	1	1.0063	3	1.0188
	1503–1504	2	1.0125	4	1.0250	9	1.0562
	2458–896	–2	0.9875	4	1.0250	7	1.0438
	2x(814–895)	1	1.0063	2	1.0125	2	1.0125
	2x(839–840)	1	1.0063	2	1.0125	–5	0.9688
	898–848	2	1.0125	2	1.0125	–3	0.9812
	934–933	–3	0.9812	–3	0.9812	–1	0.9938
	3x(939–938)	–3	0.9812	–1	0.9938	1	1.0063
	2x(960–959)	0	1.0000	0	1.0000	–1	0.9938
	2x(965–964)	–5	0.9688	–4	0.9750	–2	0.9875
T = 3	3x(1210–976)	3	1.0188	4	1.0250	7	1.0438
	1503–1504	3	1.0188	4	1.0250	5	1.0313
	2458–896	–1	0.9938	0	1.0000	1	1.0063
	2x(814–895)	–4	0.9750	–1	0.9938	3	1.0188
	2x(839–840)	–3	0.9812	–2	0.9875	11	1.0688
	898–848	–13	0.9187	–10	0.9375	–4	0.9750
	934–933	–5	0.9688	–2	0.9875	0	1.0000
	3x(939–938)	–1	0.9938	2	1.0125	6	1.0375
	2x(960–959)	–8	0.9500	–6	0.9625	–4	0.9750
	2x(965–964)	2	1.0125	3	1.0188	10	1.0625
T = 4	3x(1210–976)	–4	0.9750	–6	0.9625	–1	0.9938
	1503–1504	–1	0.9938	2	1.0125	9	1.0562
	2458–896	0	1.0000	0	1.0000	5	1.0313

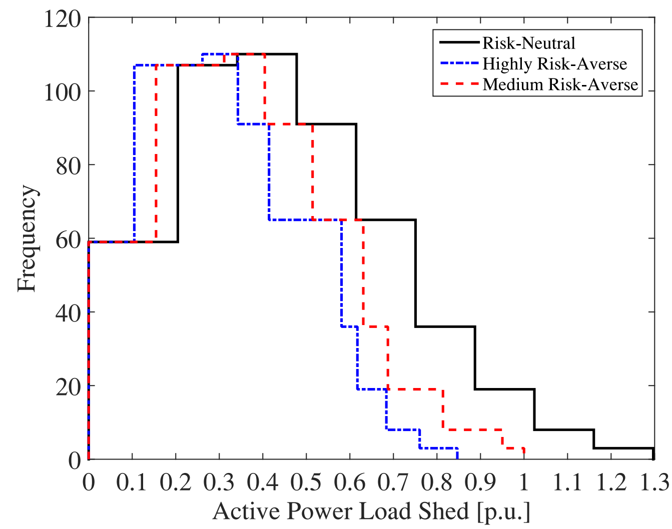

Fig. 4. Total cost distribution function for risk-neutral, highly risk-averse and medium risk-averse settings.

C. *Out-of-Sample Analysis*

We have performed a Monte Carlo simulation in order to check the reliability of the solutions for three approaches. The first approach is a risk-neutral model, i.e., we solve the proposed model considering objective $f_1(\cdot)$. The second and third approaches are highly risk-averse and medium risk-averse, respectively. For the second approach, we solve the proposed model considering the risk term only, $f_2(\cdot)$. Finally, the third approach, minimizes the equally-weighted sum of objective functions $f_1(\cdot)$ and $f_2(\cdot)$.

After running each approach, we have generated 500 demand scenarios assuming a Gaussian distribution. The optimal operation for the given VAr capacity expansion obtained from the risk-neutral solution is calculated for each generated scenario. Therefore, equations (25)–(32), are solved in the second stage for each load demand scenario. The resulting distribution functions for the active power load shedding in the risk-neutral, highly risk-averse and medium risk-averse cases are represented in Fig. 4.

For the highly risk-averse and medium risk-averse cases, the expected active load shedding represents reductions of 29% and 16%, respectively from the risk-neutral case. However, in the worst scenarios, these reductions in the active load shedding lead to a decrease from 1.3 p.u. to 0.85 p.u., representing a reduction of 34.61% for the highly risk-averse case, and from 1.3 p.u to 1 p.u., representing a reduction of 23.10% for the medium risk-averse case. Note that by means of the min-max regret paradigm, power system reliability can be improved, reducing the expected load shedding and the load shedding in the worst-case scenarios.

VI. CONCLUSION

In this paper we have solved a reactive power planning problem using a robust multi-objective mixed-integer convex formulation. The transmission expansion planner can make reasonable decisions based on robust solutions by means of a min-max regret paradigm in each expansion plan along the planning horizon. An ϵ-constraint method have been proposed to eficiently find the set of the Pareto optimal solutions. The proposed approach does not impose any limitation on the number of objectives, therefore, its extension to include more objectives (e.g. active power loss, active power generation cost, etc.) is a straightforward process.

Results show that the proposed approach is effective and flexible, producing a set of global optimum efficient frontier solutions, which allows more flexibility in the planning process in contrast to single objective methods.

The proposed approach opens several possibilities to formulate the VAr problem considering other sources as discrete reactive power sources with wind generation to analyze their impact. The proposed formulation could be helpful for transmission expansion planners in any situation where reactive power management is needed.

References

[1] V. Ajjarapu, P. L. Lau, and S. Battula, "An optimal reactive power planning strategy against voltage collapse," *IEEE Trans. Power Syst.*, vol. 9, no. 2, pp. 906–917, May 1994.

[2] G. Opoku, "Optimal power system VAr planning," *IEEE Trans. Power Syst.*, vol. 5, no. 1, pp. 53–60, Feb. 1990.

[3] N. Yorino, E. E. El-Araby, H. Sasaki, and S. Harada, "A new formulation for FACTS allocation for security enhancement against voltage collapse," *IEEE Trans. Power Syst.*, vol. 18, no. 1, pp. 3–10, Feb. 2003.

[4] S. Granville, M. V. F. Pereira, and A. Monticelli, "An integrated methodology for VAr sources planning," *IEEE Trans. Power Syst.*, vol. 3, no. 2, pp. 549–557, May 1988.

[5] B. Gorenstin, N. Campodonico, J. da Costa, and M. V. F. Pereira, "Power system expansion planning under uncertainty," *IEEE Trans. Power Syst.*, vol. 8, no. 1, pp. 129–136, Feb. 1993.

[6] E. Løken, "Use of multicriteria decision analysis methods for energy planning problems," *Renew. Sustain. Energy Rev.*, vol. 11, no. 7, pp. 1584–1595, Sep. 2007.

[7] I. Pérez Abril and J. A. G. Quintero, "VAr compensation by sequential quadratic programming," *IEEE Trans. Power Syst.*, vol. 18, no. 1, pp. 36–41, Feb. 2003.

[8] M. K. Mangoli, K. Y. Lee, and Y. M. Park, "Optimal long-term reactive power planning using decomposition techniques," *Elect. Power Syst. Res.*, vol. 26, no. 1, pp. 41–52, Jan. 1993.

[9] D. Chattopadhyay and B. Chakrabarti, "Reactive power planning incorporating voltage stability," *Int. J. Elect. Power Energy Syst.*, vol. 24, no. 3, pp. 185–200, Mar. 2002.

[10] K. Y. Lee and F. F. Yang, "Optimal reactive power planning using evolutionary algorithms: a comparative study for evolutionary programming, evolutionary strategy, genetic algorithm, and linear programming," *IEEE Trans. Power Syst.*, vol. 13, no. 1, pp. 101–108, Feb. 1998.

[11] Y. L. Chen and Y. L. Ke, "Multi-objective VAr planning for large-scale power systems using projection-based two-layer simulated annealing algorithms," *Inst. Elect. Eng. Proc. Gener., Transm. Distrib.*, vol. 151, no. 4, pp. 555–560, Jul. 2004.

[12] A. Rabiee, H. Shayanfar, and N. Amjady, "Multiobjective clearing of reactive power market in deregulated power systems," *Appl. Energy*, vol. 86, no. 9, pp. 1555–1564, Sep. 2009.

[13] S. Ramesh, S. Kannan, and S. Baskar, "Application of modified NSGA-II algorithm to multi-objective reactive power planning," *Appl. Soft Comput.*, vol. 12, no. 2, pp. 741–753, Feb. 2012.

[14] R. A. Jabr, N. Martins, B. C. Pal, and S. Karaki, "Contingency constrained VAr planning using penalty successive conic programming," *IEEE Trans. Power Syst.*, vol. 27, no. 1, pp. 545–553, Feb. 2012.

[15] N. Yang, C. W. Yu, F. Wen, and C. Y. Chung, "An investigation of reactive power planning based on chance constrained programming," *Int. J. Elect. Power Energy Syst.*, vol. 29, no. 9, pp. 650–656, Nov. 2007.

[16] J. C. López, J. Contreras, J. I. Muñoz, and J. R. S. Mantovani, "A multistage stochastic non-linear model for reactive power planning under contingencies," *IEEE Trans. Power Syst.*, vol. 28, no. 2, pp. 1503–1514, May 2013.

[17] J. C. López, D. Pozo, J. Contreras, and J. R. S. Mantovani, "A convex chance-constrained model for reactive power planning," *Int. J. Elect. Power Energy Syst.* vol. 71, pp. 403–411, Oct. 2015.

[18] Y.-T. Hsiao, H.-D. Chiang, C.-C. Liu, and Y.-L. Chen, "A computer package for optimal multi-objective var planning in large scale power systems," *IEEE Trans. Power Syst.*, vol. 9, no. 2, pp. 668–676, May 1994.

[19] Y.-L. Chen and C.-C. Liu, "Optimal multi-objective var planning using an interactive satisfying method," *IEEE Trans. Power Syst.*, vol. 10, no. 2, pp. 664–670, May 1995.

[20] R. A. Jabr, "Optimization of AC transmission system planning," *IEEE Trans. Power Syst.*, vol. 28, no. 3, pp. 2779–2787, Aug. 2013.

[21] D. Molzahn, J. Holzer, B. Lesieutre, and C. DeMarco, "Implementation of a large-scale optimal power flow solver based on semidefinite programming," *IEEE Trans. Power Syst.*, vol. 28, no. 4, pp. 3987–3998, Nov. 2013.

[22] B. Chen, J. Wang, L. Wang, Y. He, and Z. Wang, "Robust optimization for transmission expansion planning: Minimax cost vs. minimax regret," *IEEE Trans. Power Syst.*, vol. 29, no. 6, pp. 3069–3077, Nov. 2014.

[23] A. Street, F. Oliveira, and J. Arroyo, "Contingency-constrained unit commitment with $n - k$ security criterion: A robust optimization approach," *IEEE Trans. Power Syst.*, vol. 26, no. 3, pp. 1581–1590, Aug. 2011.

[24] R. Jiang, J. Wang, and Y. Guan, "Robust unit commitment with wind power and pumped storage hydro," *IEEE Trans. Power Syst.*, vol. 27, no. 2, pp. 800–810, May 2012.

[25] H. Ye and Z. Li, "Robust security-constrained unit commitment and dispatch with recourse cost requirement," *IEEE Trans. Power Syst.*, vol. 31, no. 5, pp. 3527–3536, Sep. 2016.

[26] D. Bertsimas, E. Litvinov, X. Sun, J. Zhao, and T. Zheng, "Adaptive robust optimization for the security constrained unit commitment problem," *IEEE Trans. Power Syst.*, vol. 28, no. 1, pp. 52–63, Feb. 2013.

[27] R. Jiang, J. Wang, M. Zhang, and Y. Guan, "Two-stage minimax regret robust unit commitment," *IEEE Trans. Power Syst.*, vol. 28, no. 3, pp. 2271–2282, Aug. 2013.

[28] D. E. Bell, "Regret in decision making under uncertainty," *Oper. Res.*, vol. 30, no. 5, pp. 961–981, Apr. 1982.

[29] S. Granville, J. C. O. Mello, and A. C. G. de Melo, "Application of interior point methods to power flow unsolvability," *IEEE Trans. Power Syst.*, vol. 11, no. 2, pp. 1096–1103, May 1996.

[30] R. A. Jabr, "Optimization of reactive power expansion planning," *Elect. Power Compon. Syst.*, vol. 39, no. 12, pp. 1285–1301, Feb. 2011.

[31] R. A. Jabr, "Optimal power flow using an extended conic quadratic formulation," *IEEE Trans. Power Syst.*, vol. 23, no. 3, pp. 1000–1008, Aug. 2008.

[32] D. Pozo and J. Contreras, "Finding multiple Nash equilibria in pool-based markets: A stochastic EPEC approach," *IEEE Trans. Power Syst.*, vol. 26, no. 3, pp. 1744–1752, Aug. 2011.

[33] J. L. Cohon, *Multiobjective programming and planning*, vol. 140. New York, NY, USA: Dover, 2004.

[34] G. Mavrotas and K. Florios, "An improved version of the augmented ϵ-constraint method (AUGMECON2) for finding the exact Pareto set in multi-objective integer programming problems," *Appl. Math. Comput.*, vol. 219, no. 18, pp. 9652–9669, May 2013.

[35] Sistemas teste brasileiros para uso didático e análise computacional de SEP, Federal Fluminense University, Niterio, Brazil, 2011. [Online]. Available: http://www.sistemas-teste.com.br/. Accessed on: Jan. 12, 2015.

[36] A. Olsson, G. Sandberg, and O. Dahlblom, "On Latin hypercube sampling for structural reliability analysis," *Struct. Safety*, vol. 25, no. 1, pp. 47–68, Jan. 2003.

[37] *IBM ILOG CPLEX V12.1 Users Manual for CPLEX*, IBM, Armonk, NY, USA, 2009.

[38] R. Fourer, D. M. Gay, and B. W. Kernighan, *AMPL: A Modeling Language for Mathematical Programming*. Pacific Grove, CA, USA: Duxbury, Nov. 2002.

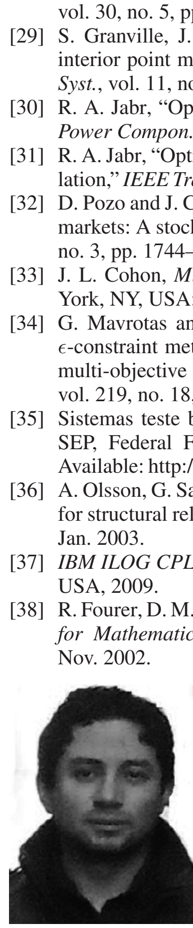

Julio López (GM'09–M'15) received the degree in electrical engineering from the Universidad Politécnica Salesiana, Cuenca, Ecuador, in 2003, and the M.Sc. and Ph.D. degrees in electrical engineering from the São Paulo State University, Sao Paulo, Brazil, in 2011 and 2014, respectively. He was a Postdoctoral Researcher in electrical engineering at the São Paulo State University in 2015.

He is currently a Full Professor in the Departamento de Inegniería Electrica, Electrónica y Telecomunicaciones, Faculty of Engineering, University of Cuenca, Cuenca, Ecuador. His research interests include the development and application of optimization techniques for the control, planning, operation, and economics of electric power systems.

David Pozo (S'09) received the B.S. and Ph.D. degrees in electrical engineering from the University of Castilla-La Mancha, Ciudad Real, Spain, in 2006 and 2013, respectively.

He is currently a Research Fellow in the Department of Electrical Engineering, Pontifical Catholic University of Rio de Janeiro, Rio de Janeiro, Brazil. His research interests include power systems economics and electricity markets.

Javier Contreras (SM'05–F'15) received the B.S. degree in electrical engineering from the University of Zaragoza, Zaragoza, Spain, in 1989, the M.Sc. degree from the University of Southern California, Los Angeles, CA, USA, in 1992, and the Ph.D. degree from the University of California, Berkeley, CA, USA, in 1997.

He is currently a Professor at the Universidad de Castilla-La Mancha, Ciudad Real, Spain. His research interests include power systems planning, operations, and economics, as well as electricity markets.

Jose Roberto Sanches Mantovani (M'03) received the electrical engineer degree from São Paulo State University, Sao Paulo, Brazil, in 1981, and the M.Sc. and Ph.D degrees in electrical engineering from the University of Campinas, São Paulo, Brazil, in 1987 and 1995, respectively. From 2006 to 2007, he was with the Department of Electrical and Computer Engineering, University of Illinois, Chicago, IL, USA. He is currently an Associate Professor in Laboratorio de Planejamento de Sistemas de Energia Eletrica, Department of Electrical Engineering, São Paulo State University.